GEOPHYSICAL RESEARCH LETTERS, VOL. 39, L02807, doi:10.1029/2011GL050099, 2012

Effects of amines on formation of sub-3 nm particles and their subsequent growth

Huan Yu,[1] Robert McGraw,[2] and Shan-Hu Lee[1]

Received 25 October 2011; revised 17 December 2011; accepted 28 December 2011; published 28 January 2012.

[1] Field observations and quantum chemical calculations suggest that amines can be important for formation of nanometer size particles. Amines and ammonia often have common atmospheric emission sources and the similar chemical and physical properties. While the effects of ammonia on aerosol nucleation have been previously investigated, laboratory studies of homogeneous nucleation involving amines are lacking. We have made kinetics studies of multicomponent nucleation (MCN) with sulfuric acid, water, ammonia and amines under conditions relevant to the atmosphere. Low concentrations of aerosol precursors were measured with chemical ionization mass spectrometers (CIMS) to provide constrained precursor concentrations needed for nucleation. Particle sizes larger than ~2 nm were measured with a nano-differential mobility analyzer (nano-DMA), and number concentrations of particles larger than ~1 nm were measured with a particle size magnifier (PSM). Our observations provide the laboratory evidence that amines indeed can participate in aerosol nucleation and growth at the molecular cluster level. The enhancement of particle number concentrations due to several atmospherically relevant amine compounds and ammonia were related to the basicity of these compounds, indicating that acid–base reactions may contribute to the formation of sub-3 nm particles. **Citation:** Yu, H., R. McGraw, and S.-H. Lee (2012), Effects of amines on formation of sub-3 nm particles and their subsequent growth, *Geophys. Res. Lett.*, *39*, L02807, doi:10.1029/2011GL050099.

1. Introduction

[2] Atmospheric nucleation is an important source of new aerosol particles which may significantly contribute to the global production of cloud condensation nuclei (CCN) [*Merikanto et al.*, 2009]. Ultrafine particles also have adverse effects on human health. But at present, the nucleation mechanisms are poorly understood. Recent chemical analysis of nanoparticles showed that nanometer size particles contain sulfate and ammonium, along with various oxygen- and nitrogen-containing organic components in a wide range of atmospheric conditions, from rural to urban areas and from biogenic to polluted environments [*Bzdek et al.*, 2011; *Makela et al.*, 2001; *Smith et al.*, 2010]. Molecular clusters containing H_2SO_4 and amines were also observed in the atmosphere [*Zhao et al.*, 2011].

[3] Quantum chemical calculations showed that amines can form neutral and ion clusters with H_2SO_4, even more effectively than NH_3 [*Kurtén et al.*, 2008] and that amines can stabilize H_2SO_4 dimers to prevent evaporation of these dimers [*Petaja et al.*, 2011]. Laboratory studies further showed that amines can substitute ammonium to aminium in sub-3 nm aerosol particles [*Bzdek et al.*, 2010]. However, there are so far only two laboratory studies that have examined the effects of trimethylamine and tert-butylamine on H_2SO_4 aerosol nucleation [*Berndt et al.*, 2010; *Erupe et al.*, 2011].

[4] Here, we have investigated the H_2SO_4-amine-H_2O multi-component nucleation system (MCN) in a fast flow nucleation reactor coupled with a particle sizing magnifier (PSM), a butanol-based ultrafine condensation particle counter (CPC), a nano-differential mobility analyzer (nano-DMA), and two chemical ionization mass spectrometers (CIMS). The PSM, coupled with a CPC, can count particles as small as ~1 nm [*Vanhanen et al.*, 2011], thus including those newly formed molecular clusters. Two CIMSs were used to measure low concentrations of H_2SO_4, NH_3, and amines with fast time response. To our best knowledge, currently we are the only group that is making simultaneous measurements of these acid and base precursor compounds for nucleation studies. Five atmospherically most relevant amine compounds (methylamine, dimethylamine, trimethylamine, triethylamine, and tert-butylamine) were investigated and the enhancement of nucleation due to amines was compared to NH_3.

2. Experiments

[5] The Kent State University nucleation experiment system consists of four components: an OH generator, a mixing tube, a transit tube, and a fast flow nucleation tube attached to two CIMSs and particle detectors. The setup has been described in detail elsewhere [*Benson et al.*, 2009, 2008, 2011; *Erupe et al.*, 2011; *Young et al.*, 2008]. Figure S1 in the auxiliary material shows the experimental conditions used in the present study, including flow tube dimension, flow rate, residence time, and temperature.[1]

[6] In the mixing tube the distance between the two ports, where SO_2 and amine were introduced, was 16.4 cm (residence time 6.2 s) (Figure S1). This relatively long distance was used to minimize the amine oxidation by OH; hence with this configuration, the CIMS-measured [H_2SO_4] at the end of the mixing tube did not decrease, even when very high concentrations of dimethylamine (e.g., 20 ppbv) were introduced. A high temperature (318 ± 5 K) was also applied to the mixing tube to prevent nucleation of H_2SO_4. This allowed the gas phase H_2SO_4 molecules (without being nucleated) to be merged with amines, before entering the cooler

[1]College of Public Health, Kent State University, Kent, Ohio, USA.
[2]Atmospheric Science Division, Brookhaven National Laboratory, Upton, New York, USA.

0094-8276/12/2011GL050099

[1]Auxiliary materials are available in the HTML. doi:10.1029/2011GL050099.

Table 1. Concentrations of Impurity NH_3, Methylamine, Dimethylamine, and Trimethylamine in the Nucleation System Detected by Chemical Ionization Mass Spectrometer (CIMS), From Several Possible Sources Including Water Vapor, the N_2 Gas Vaporized From Liquid Nitrogen, and Different Amine Permeation Tubes[a]

Impurities Detected	Detection Limit (pptv)	From Water Vapor (pptv)		From Liquid Nitrogen Gas (pptv)	From Methylamine Permeation Tube (pptv per ppbv)	From Dimethylamine Permeation Tube (pptv per ppbv)	From Trimethylamine Permeation Tube (pptv per ppbv)	Total in NLB (pptv) RH < 70%
		RH 32%	RH 70%					
NH_3[b]	54	BDL	84 ± 17	BDL	76 ± 6	BDL	BDL	<84 ± 17
methylamine[c]	14	BDL	BDL	BDL	-	BDL	BDL	BDL
dimethylamine[d]	75	BDL	BDL	BDL	BDL	-	BDL	BDL
trimethylamine[e]	8	BDL	32 ± 3	BDL	BDL	BDL	-	<32 ± 3

[a]The impurity concentrations measured from the permeation tubes are shown here as pptv impurity concentrations in 1 ppbv amine in the nucleation tube. Impurity concentrations were also determined for the NLB "Nucleation occurring with Low concentrations of impurity Base compounds". Ion-chemical reaction schemes used in CIMS to detect each of these base molecules and their detection limits (with 1 minute integration time) are also indicated. BDL indicates below the detection limit of CIMS.

[b]For the NH_3 detection, the following reaction scheme was used: $(C_2H_5OH)_nH^+ + NH_3 \rightarrow NH_3(C_2H_5OH)_{n-m}H^+ + m(C_2H_5OH)$, where n and m = 1, 2, 3… etc. and m ≤ n, based on [*Benson et al.*, 2010].

[c]For the methylamine detection: $(C_2H_5OH)_nH^+ + (CH_3)NH_2 \rightarrow (CH_3)NH_2{\cdot}(C_2H_5OH)_{n-m}H^+ + m(C_2H_5OH)$.

[d]For the dimethylamine detection: $(CH_3COCH_3)_nH^+ + (CH_3)_2NH \rightarrow (CH_3)_2NH{\cdot}(CH_3COCH_3)_{n-m}H^+ + m(CH_3COCH_3)$. This ion reagent was chosen to avoid the two nascent peaks, $(CH_3)_2NH{\cdot}H^+$ (m/z = 46) and $(C_2H_5OH)H^+$ (m/z = 47).

[e]For the trimethylamine detection: $(C_2H_5OH)_nH^+ + (CH_3)_3N \rightarrow (CH_3)_3N{\cdot}(C_2H_5OH)_{n-m}H^+ + m(C_2H_5OH)$ [*Erupe et al.*, 2011].

nucleation reactor (287 K). Under typical experimental conditions, a total flow of 8.26 liters per minute (lpm) passed through from the hot mixing tube; amongst, 5 lpm was introduced into to CIMS attached to the beginning of the nucleation reactor, and the rest to the nucleation reactor.

[7] The detection limit of our H_2SO_4-CIMS is ~5 × 10^4 cm^{-3} with an integration time of 1 minute [*Benson et al.*, 2009, 2008; *Erupe et al.*, 2010]. NH_3 and amine concentrations were estimated based on the concentrations determined using pre-calibrated, National Institute of Standard and Technology (NIST) traceable permeation tubes in a gas standard generator (Kin-Tek 491 MB), combined with further dilution ratios in the mixing tube. Concentrations of impurity NH_3 and amines in the flow tube system were also systematically investigated with CIMS based on [*Benson et al.*, 2010; *Erupe et al.*, 2011] (Table 1). The detection limit (3 standard deviations of the background signal fluctuation) of our CIMS for NH_3, methylamine, dimethylamine, and trimethylamine is 54, 14, 75, and 8 pptv, respectively, with an integration time of 1 minute (Table 1). Table 1 summarizes the ion molecule reaction schemes used for the detection of these compounds, as well as the measured impurity levels of each compound originated from water vapor, carrier gases, and amine permeation tubes. Our results indicate that water vapor was the major contamination source of these base impurities, while the impurity NH_3 and amines from the carrier gases were all below the detection limits. When no ternary species was introduced into the nucleation reactor, the detected NH_3 and trimethylamine impurities were 84 ± 17 pptv (one standard deviation in the measurements) and 32 ± 3 pptv, respectively, at RH of 70%. At RH of 32%, these base compounds were all below the detection limit. Due to these impurities, the experiments performed without adding ternary species, which was intended to represent the binary homogeneous nucleation (BHN) system, were referred to as the "Nucleation with Low concentrations of impurity Base compounds (NLB)". The experiments performed with the addition of base compounds were referred to as multicomponent nucleation (MCN). Thus, the enhancement factors (*EF*, the ratio of total particle number concentrations measured with the addition of base compounds vs. without adding them) obtained in the present study may be considered as the lower limit of the actual enhancement by base compounds.

[8] A PSM and a butanol-CPC (TSI 3776) were used to measure particle number concentrations. The detection efficiency of TSI 3776 is 100% at 3 nm, 50% at 2.3 nm, 25–30% at 2 nm and ~10% at ~1.8 nm, respectively, (http://tsi.com/uploadedFiles/Product_Information/Literature/Spec_Sheets/3776_2980345.pdf).

[9] The detection efficiency of PSM is ~100% at 3 nm, 50% at 1.5 nm, and ~37% at 1 nm, with a flow rate of 1.0 lpm of the diethylene glycol saturator [*Vanhanen et al.*, 2011]. Particle sizes from ~2–100 nm were measured with nano-DMA (TSI 3085) using a high flow rate (1.5 lpm) of the CPC butanol saturator, for relatively large particles produced under high [H_2SO_4] conditions (>10^8 cm^{-3}). An inversion program was also developed to estimate size distributions of particles based on the number concentrations measured with PSM, as described in Section 3. This inversion method was used to predict size distributions of small particles (<2 nm), typically formed at [H_2SO_4] from 10^6–10^7 cm^{-3} with a short residence time (34 s).

[10] The nucleation zone was determined experimentally using a moveable injector, similar to [*Ball et al.*, 1999], by measuring particle number concentrations along the axis of the nucleation reactor (5.08 cm i.d. and 90 cm long, corresponding to 34 s residence time) (Figure S2a). At the very beginning of the nucleation reactor, there was a negligible number of particles. Particle number concentrations then increased with axial distance and leveled off at 52 ± 3 cm (corresponding to a nucleation time of ~19.4 s). This measured nucleation zone was also consistent with numerical calculations of a nucleation inversion model showing that nucleation time is about half of the residence time in the nucleation tube [*Young et al.*, 2008]. Figure S2b shows the time evolution of H_2SO_4 and dimethylamine concentrations and total number concentrations of particles in the nucleation tube under the typical experimental conditions.

3. Results and Discussion

[11] Particle size distributions in the diameter range from 0.5 to 5 nm were estimated from the measured PSM number

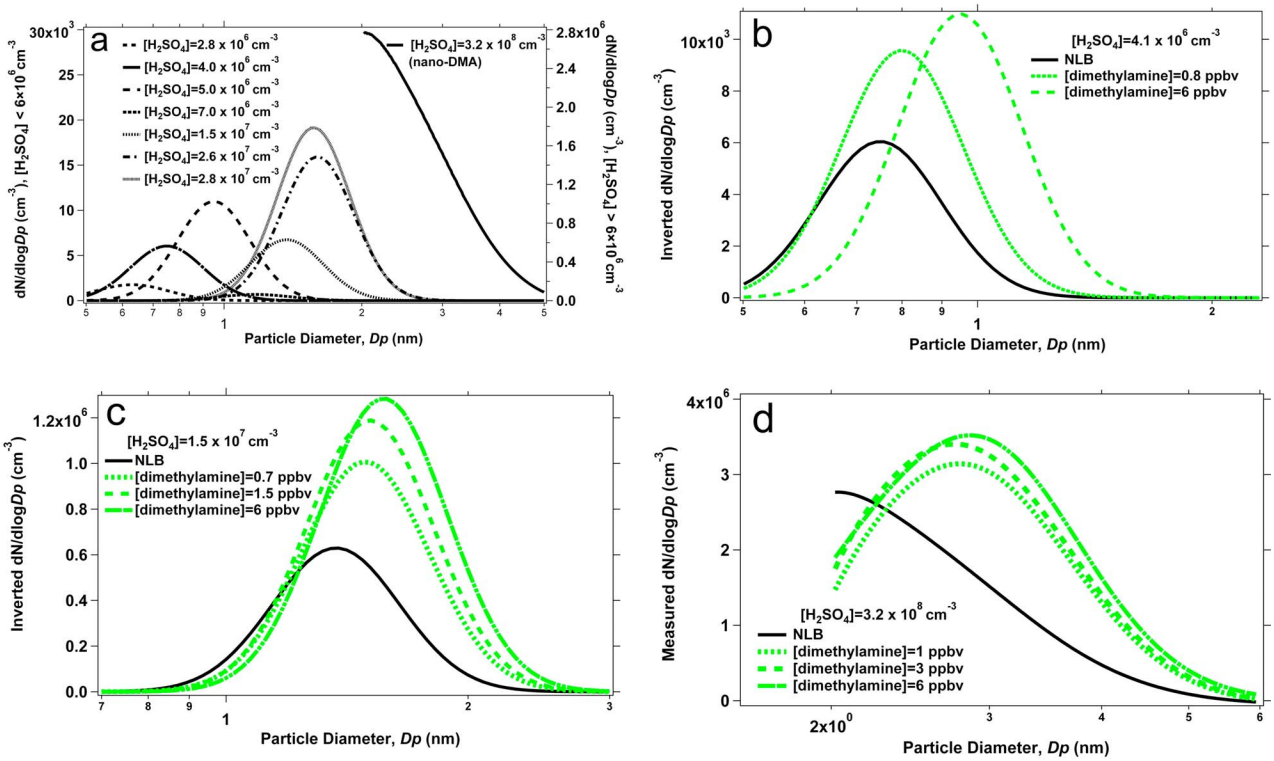

Figure 1. (a) The inverted particle size distributions from the PSM measurements for NLB (without adding ternary species but under the influence of low concentrations of base compounds) at $[H_2SO_4]$ from 3×10^6–3×10^7 cm^{-3} and RH of 32%. In comparison, the nano-DMA measured size distribution at $[H_2SO_4]$ of 3×10^8 cm^{-3} is also included here. Note that two different Y axis scales are used for different $[H_2SO_4]$ ranges. (b) The inverted particle size distributions for NLB (black) and MCN (multicomponent nucleation) with dimethylamine (green) at $[H_2SO_4]$ of 4×10^6 cm^{-3} and RH of 32%. (c) The same as Figure 1b, except that $[H_2SO_4] = 2 \times 10^7$ cm^{-3}. (d) The particle size distributions measured with nano-DMA (TSI 3085) for NLB (black) and MCN with dimethylamine (green) at $[H_2SO_4]$ of 3×10^8 cm^{-3} and RH of 70%. Table S1 shows the PSM-measured number concentrations, the inverted particle median diameters and the inverted total number concentrations, for the data shown in this figure.

concentrations with an inversion program which we have developed based on that of *Brock et al.* [2000]. The PSM detection efficiencies of particles in the size range from 1 to 5 nm were obtained using the mobility standard tetrapropyl ammonium halides and the positively charged silver nanoparticles, with saturator flow rates of 0.6 lpm, 0.8 lpm, and 1.0 lpm. Detection efficiencies of particles in the size range from 0.5 to 1 nm were extrapolated from the measured calibration curve. Particles generated in the nucleation tube, likely containing H_2SO_4, sulfate, ammonium, and aminium, were assumed to have the same detection efficiencies as the calibration particles. The detection efficiency of calibration particles has taken into account the diffusion loss inside the PSM. The sampling inlet between the PSM and the nucleation tube was only 4 cm (0.56 cm I.D.), so the diffusion loss in the sampling inlet was assumed to be minimal. Particles larger than 3 nm produced in the fast flow nucleation reactor were previously found to be in lognormal size distribution when measured with a nano-DMA [*Benson et al.*, 2008], so particles smaller than 3 nm were also assumed to be in the lognormal size distribution. A nonlinear least-square regression method was used to optimize the size distribution. Uncertainties associated with the inversion include uncertainties in the detection efficiency, differences in the detection efficiency for the calibration and the measured particles, and uncertainties in the extrapolated calibration curve. Sensitivity analysis made by perturbing the detection efficiencies up to ±20% bias showed that the inverted particle median diameters varied within ±10% and the inverted total particle number concentrations varied within ±17%.

[12] Figure 1a shows the inverted particle size distributions for NLB (that is, nucleation occurring without adding ternary species but under the influence of low concentrations of impurity base compounds) at RH of 32%. In comparison, the particle size distribution measured with nano-DMA at $[H_2SO_4]$ of 3×10^8 cm^{-3} is also included. With increasing $[H_2SO_4]$ (from 3×10^6 cm^{-3} to 3×10^7 cm^{-3}), the inverted particle median sizes ($D_{p,invt}$) and the inverted total number concentrations (N_{invt}) both increased dramatically. For example, $D_{p,invt}$ was 0.6 nm and N_{invt} was 350 cm^{-3} at $[H_2SO_4]$ of 3×10^6 cm^{-3}, whereas $D_{p,invt}$ was 1.6 nm and N_{invt} was 4×10^5 cm^{-3} at $[H_2SO_4]$ of 3×10^7 cm^{-3} (Table S1). Thus, when $[H_2SO_4]$ increased with one order of magnitude, $D_{p,invt}$ increased with a factor of 2.5 and N_{invt} increased with 3 orders of magnitude, indicating the significant effect of H_2SO_4 on aerosol nucleation and growth for sub−3 nm particles.

[13] Figures 1b and 1c show the inverted size distributions in NLB and dimethylamine-MCN, as a function of aerosol precursor concentrations. Compared to the NLB (at $[H_2SO_4]$

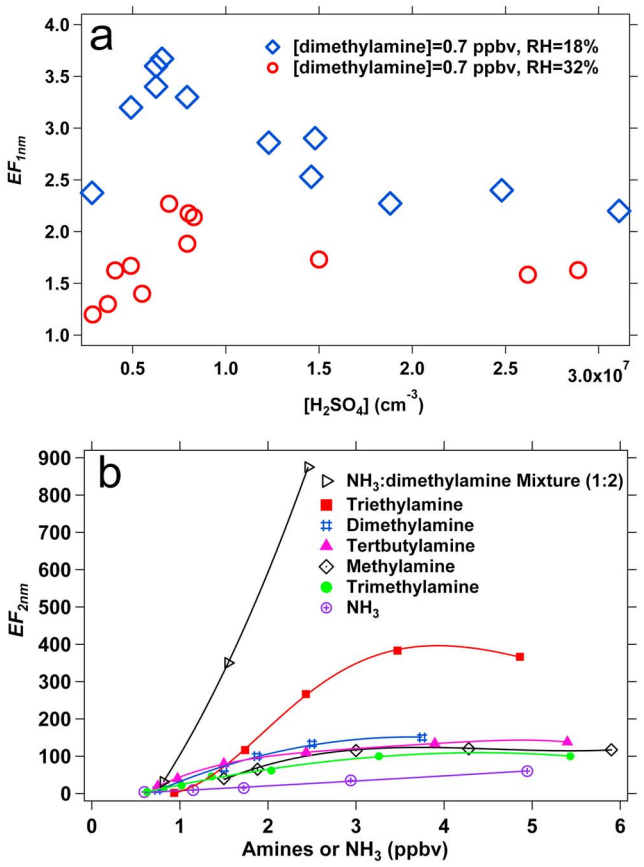

Figure 2. (a) The EF_{1nm} (derived from the number concentrations of particles larger than 1 nm measured with PSM, N_{1nm}) due to [dimethylamine] of 0.7 ppbv at $[H_2SO_4]$ from 3×10^6–3×10^7 cm^{-3} and RH of 18% (diamonds) and 32% (circles). (b) The EF_{2nm} (derived from the number concentrations of particles larger than 2 nm measured with TSI 3776, N_{2nm}) due to several atmospherically relevant amines, NH_3, and a mixture of dimethylamine and NH_3.

of 4×10^6 cm^{-3}), $D_{p,invt}$ increased with a factor of 1.3 and N_{invt} increased with a factor of 1.7 when dimethylamine of 6 ppbv was added (Table S1). However, both $D_{p,invt}$ and N_{invt} did not increase further, when [dimethylamine] was higher than 6 ppbv. This trend found at low $[H_2SO_4]$ (10^6–10^7 cm^{-3}) was also consistent with the nano-DMA measurements made at high $[H_2SO_4]$ (e.g., 3×10^8 cm^{-3}), where the measured particle median size ($D_{p,meas}$) increased with a factor of 1.4 and the total number concentration of particles (N_{meas}) increased with a factor of 1.6 with [dimethylamine] of 6 ppbv (Figure 1d). These results indicate that dimethylamine indeed can enhance both the sizes and total particle number concentrations of particles, demonstrating that dimethylamine can promote the formation of sub-3 nm particles and their subsequent growth. However, the comparison between NLB (Figure 1a) and MCN size distributions (Figures 1b–1d) also indicates that H_2SO_4 has a more dominant effect on particle sizes and number concentrations of sub-3 nm particles, compared to dimethylamine.

[14] We have examined the dependence of enhancement effect (*EF*) on $[H_2SO_4]$ and RH. These *EF* values (EF_{1nm}) were derived from the number concentrations of particles larger than ~1 nm (N_{1nm}) measured with PSM (Figure 2a). At $[H_2SO_4]$ from 3×10^6–3×10^7 cm^{-3}, the EF_{1nm} due to dimethylamine (0.7 ppbv) ranged from 2–4 at RH of 18%, and EF_{1nm} ranged from 1–2.5 at RH of 32%. The EF_{1nm} curves at these two RH conditions followed the same trend: EF_{1nm} increased with increasing $[H_2SO_4]$ at $[H_2SO_4] < 7 \times 10^6$ cm^{-3} and EF_{1nm} decreased with increasing $[H_2SO_4]$ at $[H_2SO_4] > 7 \times 10^6$ cm^{-3}. Previous laboratory investigations have also showed that enhancement due to NH_3 [*Ball et al.*, 1999; *Benson et al.*, 2009; *Zhao et al.*, 2011] and trimethylamine [*Erupe et al.*, 2011] decreases with increasing $[H_2SO_4]$ at $[H_2SO_4] > 1 \times 10^8$ cm^{-3}. The different trends of EF_{1nm} seen at different $[H_2SO_4]$ conditions suggest that nucleation was in transition from the H_2SO_4-limited ($[H_2SO_4] < 7 \times 10^6$ cm^{-3}) to the amine-limited regime ($[H_2SO_4] > 7 \times 10^6$ cm^{-3}), under our experimental conditions with a residence time of 34 s.

[15] Figure 2b shows the measured *EF* due to methylamine, dimethylamine, trimethylamine, triethylamine, tert-butylamine and NH_3 at $[H_2SO_4]$ of 7×10^6 cm^{-3} and RH of 32%. The *EF* (EF_{2nm}) values shown here were estimated from the number concentrations of particles larger than ~2 nm (N_{2nm}) measured with TSI 3776 CPC. These EF_{2nm} values (10–400) were much higher than EF_{1nm} (1–4) (Figure 2a). This was because of the particle growth due to amines. For example, at $[H_2SO_4]$ of 7×10^6 cm^{-3} without dimethylamine, N_{invt} was 1.1×10^4 cm^{-3} with $D_{p,invt}$ of 1.2 nm, while N_{2nm} was only ~20 cm^{-3} (Figure 1a). With the addition of dimethylamine of 3 ppbv, N_{invt} increased slightly to 2×10^4 cm^{-3}, but $D_{p,invt}$ shifted to a much larger size (1.4 nm) which resulted in a higher N_{2nm} of ~2000 cm^{-3}. As a result, the EF_{2nm} was derived to be ~100 (Figure 2b). Additionally, because the detection efficiency of TSI 3776 has a steep curve between 1.8 (~10%) and 3 nm (100%), this also contributed to the larger magnitude of EF_{2nm}.

[16] The order of EF_{2nm} due to amines and NH_3 increased from NH_3 (basicity pK_b = 4.75 [*Sorrell*, 2006]), trimethylamine (pK_b = 4.22), methylamine (pK_b = 3.35), tert-butylamine (pK_b = 3.32), dimethylamine (pK_b = 3.27), to triethylamine (pK_b = 3.25) (Figure 2b), consistent with the order of basicity of these base compounds. The order of basicity of amine molecules is determined by the number and the size of the alkyl substituent, except that trimethylamine has a lower basicity due to the steric effect from three methyl groups. Recent quantum chemical calculations also suggested that dimethylamine-containing clusters can be thermodynamically more stable than trimethylamine-containing clusters [*Kurtén et al.*, 2008; *Nadykto et al.*, 2011]. Interestingly, a mixture of dimethylamine with NH_3 (1:2 ratio in mixing ratios) was found to enhance nucleation more effectively than dimethylamine or NH_3 alone (Figure 2b). To explain this unique feature, future studies are required to investigate the thermodynamic stability of H_2O-H_2SO_4-NH_3-amine clusters.

[17] Figure S3 shows the measured Log *J* vs. Log $[H_2SO_4]$ and Log *J* vs. Log RH in NLB and dimethylamine-MCN, as well as Log *J* vs. Log [dimethylamine] in MCN. These *J* values were obtained from the PSM-measured N_{1nm}. For both NLB and MCN, the slopes of Log *J* vs. Log $[H_2SO_4]$ were around 2 (Figure S3a). The threshold $[H_2SO_4]$ required for *J* of 1 cm^{-3} s^{-1} was between 4×10^5 and 2×10^6 cm^{-3} at RH from 28–80% in NLB. With the dimethylamine, the threshold $[H_2SO_4]$ decreased slightly to 4×10^5–1×10^6 cm^{-3}. The slope of Log *J* vs. Log RH was around 1.7–2.3 for $[H_2SO_4]$ between 2×10^6 and 1×10^7 cm^{-3} for

NLB; with the dimethylamine, the slope decreased slightly to 1.3–1.6 (Figure S3b). The slope of Log J vs. Log [dimethylamine] was only ~0.2 (Figure S3c), consistent with the previous studies which showed that the slopes of Log J vs. Log [trimethylamine] [*Erupe et al.*, 2011] and Log J vs. Log [NH_3] are smaller than 1 [*Benson et al.*, 2011].

4. Conclusions

[18] We have made laboratory observations of multicomponent nucleation involving H_2SO_4 and several atmospherically relevant amines using a fast flow nucleation reactor under H_2SO_4 concentrations from 10^6–10^8 cm^{-3}, amine concentrations from 0.3–6.0 ppbv, RH from 18–80%, and a temperature of 278 K. Both particle sizes and total number concentrations of sub-3 nm particles increased with increasing H_2SO_4 and dimethylamine concentrations, indicating that dimethylamine is also involved in aerosol nucleation and growth. But the effect of H_2SO_4 on formation of sub-3 nm particles was more dominant than that of dimethylamine, indicating that H_2SO_4 is still the key nucleation precursor even in the presence of ppbv or sub-ppbv of ternary base compounds. While the enhancement due to dimethylamine on number concentrations of particles larger than ~1 nm were smaller than 5, the enhancement on particles larger than ~2 nm were on the two orders of magnitude. The order of enhancement due to methylamine, dimethylamine, trimethylamine, triethylamine, and tert-butylamine and ammonia was the same as the order of basicity of these compounds, implying that acid–base reactions may play an important role in the amine effects on H_2SO_4 aerosol nucleation.

[19] **Acknowledgments.** This study was supported by NOAA (NA08OAR4310537), NSF (Career ATM-0645567; AGS-1137821) and Ohio Board of Regents. We thank Greg Huey, Dave Tanner, Jyri Mikkilä, Chuck Brock, Barbara Wyslouzil and Vijay Kanawade for useful discussions.

[20] The Editor thanks Jim Smith and an anonymous reviewer for their assistance in evaluating this paper.

References

Ball, S. M., D. R. Hanson, F. L. Eisele, and P. H. McMurry (1999), Laboratory studies of particle nucleation: Initial results for H_2SO_4, H_2O, and NH_3 vapors, *J. Geophys. Res.*, *104*, 23,709–23,718, doi:10.1029/1999JD900411.

Benson, D. R., L. H. Young, R. Kameel, and S.-H. Lee (2008), Laboratory-measured sulfuric acid and water homogeneous nucleation rates from the SO_2 + OH reaction, *Geophys. Res. Lett.*, *35*, L11801, doi:10.1029/2008GL033387.

Benson, D. R., M. E. Erupe, and S.-H. Lee (2009), Laboratory-measured H_2SO_4-H_2O-NH_3 ternary homogeneous nucleation rates: Initial observations, *Geophys. Res. Lett.*, *36*, L15818, doi:10.1029/2009GL038728.

Benson, D. R., A. Markovich, M. Al-Refai, and S.-H. Lee (2010), A Chemical Ionization Mass Spectrometer for ambient measurements of ammonia, *Atmos. Meas. Tech.*, *3*, 1075–1087, doi:10.5194/amt-3-1075-2010.

Benson, D. R., J. H. Yu, A. Markovich, and S.-H. Lee (2011), Laboratory observations of ternary homogeneous nucleation of H_2SO_4, NH_3, and H_2O under conditions relevant to the lower troposphere, *Atmos. Chem. Phys.*, *11*, 4755–4766, doi:10.5194/acp-11-4755-2011.

Berndt, T., et al. (2010), Laboratory study on new particle formation from the reaction OH + SO_2: Influence of experimental conditions, H_2O vapour, NH_3 and the amine tert-butylamine on the overall process, *Atmos. Chem. Phys.*, *10*, 7101–7116, doi:10.5194/acp-10-7101-2010.

Brock, C. A., F. Schrorder, B. Karcher, A. Petzold, R. Busen, and M. Fiebig (2000), Ultrafine particle size distributions measured in aircraft exhaust plumes, *J. Geophys. Res.*, *105*, 26,555–26,567, doi:10.1029/2000JD900360.

Bzdek, B., D. Ridge, and M. Johnston (2010), Amine exchange into ammonium bisulfate and ammonium nitrate nuclei, *Atmos. Chem. Phys.*, *10*, 3495–3503, doi:10.5194/acp-10-3495-2010.

Bzdek, B. R., C. A. Zordan, G. W. Luther, and M. V. Johnston (2011), Nanoparticle chemical composition during new particle formation, *Aerosol Sci. Technol.*, *45*, 1041–1048, doi:10.1080/02786826.2011.580392.

Erupe, M. E., et al. (2010), Correlation of aerosol nucleation rate with sulfuric acid and ammonia in Kent, Ohio: An atmospheric observation, *J. Geophys. Res.*, *115*, D23216, doi:10.1029/2010JD013942.

Erupe, M. E., A. A. Viggiano, and S. H. Lee (2011), The effect of trimethylamine on atmospheric nucleation involving H_2SO_4, *Atmos. Chem. Phys.*, *11*, 4767–4775, doi:10.5194/acp-11-4767-2011.

Kurtén, T., V. Loukonen, H. Vehkamäki, and M. Kulmala (2008), Amines are likely to enhance neutral and ion-induced sulfuric acid-water nucleation in the atmosphere more effectively than ammonia, *Atmos. Chem. Phys.*, *8*, 4095–4103, doi:10.5194/acp-8-4095-2008.

Makela, J. M., et al. (2001), Chemical compostion of aerosol during particle formation events in boreal forest, *Tellus, Ser. B*, *53*, 380–393, doi:10.1034/j.1600-0889.2001.d01-27.x.

Merikanto, J., D. V. Spracklen, G. W. Mann, S. J. Pickering, and K. S. Carslaw (2009), Impact of nucleation on global CCN, *Atmos. Chem. Phys.*, *9*, 8601–8616, doi:10.5194/acp-9-8601-2009.

Nadykto, A. B., F. Yu, M. V. Jakovleva, J. Herb, and Y. Xu (2011), Amines in the Earth's atmosphere: A density functional theory study of the thermochemistry of pre-nucleation clusters, *Entropy*, *13*, 554–569, doi:10.3390/e13020554.

Petaja, T., M. Sipila, P. Paasonen, T. Nieminen, T. Kurten, I. K. Ortega, F. Stratmann, H. Vehkamaki, T. Berndt, and M. Kulmala (2011), Experimental observation of strongly bound dimers of sulfuric acid: Application to nucleation in the atmosphere, *Phys. Rev. Lett.*, *106*, 228302, doi:10.1103/PhysRevLett.106.228302.

Smith, J. N., K. C. Barsanti, H. R. Friedli, M. Ehn, M. Kulmala, D. R. Collins, J. H. Scheckman, B. J. Willians, and P. H. McMurry (2010), Observations of ammonium salts in atmospheric nanoparticles and possible climatic implications, *Proc. Natl. Acad. Sci. U. S. A.*, *107*, 6634–6639, doi:10.1073/pnas.0912127107.

Sorrell, T. N. (2006), *Organic Chemistry*, Univ. Sci., Sausalito, Calif.

Vanhanen, J., J. Mikkila, K. Lehtipalo, M. Sipila, H. E. Manninen, E. Siivola, T. Petaja, and M. Kulmala (2011), Particle size magnifier for nano-CN detection, *Aerosol Sci. Technol.*, *45*, 533–542, doi:10.1080/02786826.2010.547889.

Young, L. H., D. R. Benson, F. Rifkha, J. R. Pierce, H. Junninen, M. Kulmala, and S.-H. Lee (2008), Laboratory studies of sulfuric acid and water binary homogeneous nucleation: Evaluation of laboratory setup and preliminary results, *Atmos. Chem. Phys.*, *8*, 4997–5016, doi:10.5194/acp-8-4997-2008.

Zhao, J., J. N. Smith, F. L. Eisele, M. Chen, C. Kuang, and P. H. McMurry (2011), Observation of neutral sulfuric acid-amine containing clusters in laboratory and ambient measurements, *Atmos. Chem. Phys.*, *11*, 10,823–10,836, doi:10.5194/acp-11-10823-2011.

S.-H. Lee and H. Yu, College of Public Health, Kent State University, Williams Hall 303, Kent, OH 44240, USA. (slee19@kent.edu)

R. McGraw, Atmospheric Science Division, Brookhaven National Laboratory, Bldg. 815E, 75 Rutherford Dr., Upton, NY 11973, USA.